



HAL
open science

Analysis of a full discretization scheme for a 2D nonlinear coupled system of radiative-conductive heat transfer equations

Mohamed Ghattassi, Jean-Rodolphe Roche, Didier Schmitt

► **To cite this version:**

Mohamed Ghattassi, Jean-Rodolphe Roche, Didier Schmitt. Analysis of a full discretization scheme for a 2D nonlinear coupled system of radiative-conductive heat transfer equations. *Journal of Computational and Applied Mathematics*, 2019, 346, pp.1-17. 10.1016/j.cam.2018.06.028 . hal-01283667v2

HAL Id: hal-01283667

<https://hal.science/hal-01283667v2>

Submitted on 8 Feb 2019

HAL is a multi-disciplinary open access archive for the deposit and dissemination of scientific research documents, whether they are published or not. The documents may come from teaching and research institutions in France or abroad, or from public or private research centers.

L'archive ouverte pluridisciplinaire **HAL**, est destinée au dépôt et à la diffusion de documents scientifiques de niveau recherche, publiés ou non, émanant des établissements d'enseignement et de recherche français ou étrangers, des laboratoires publics ou privés.

Copyright

Analysis of a full discretization scheme for 2D radiative-conductive heat transfer systems

Mohamed GHATTASSI^{a,b}, Jean Rodolphe ROCHE^b, Didier SCHMITT^b

^a*Computer, Electrical, and Mathematical Sciences and Engineering Division, King Abdullah University of Science and Technology (KAUST), Thuwal, 53955-6900, Kingdom of Saudi Arabia.*

^b*University of Lorraine, IECL UMR CNRS 7502, 54506 Vandoeuvre-lès-Nancy, France.*

Abstract

This paper deals with the convergence of numerical scheme for combined nonlinear radiation-conduction heat transfer system in a gray, absorbing and non-scattering two-dimensional medium. The radiative transfer equation is solved using a Discontinuous Galerkin method with upwind fluxes. The conductive equation is discretized using the finite element method. Moreover, the Crank-Nicolson scheme is applied for time discretization of the semi-discrete nonlinear coupled system. Existence and uniqueness of the solution for the continuous and full discrete system are presented. The convergence proof follows from the application of a discrete fixed-point theorem, involving only the temperature fields at each time step. The order of approximation error, stability, and order of convergence are investigated. Finally, the theoretical stability and convergence results are supported with numerical examples.

Keywords: Radiative-conductive heat transfer, Galerkin method, Crank-Nicolson scheme, Banach fixed point theorem, error estimates.

Introduction

The aim of the present paper is to analyze a numerical method for nonlinear partial differential equations of radiative-conductive heat transfer system. The model considers a radiative transfer equation (RTE) coupled with a nonlinear conductive heat transfer equation (CE) in two-dimensional cases, i.e., the projection of the surface on the unit sphere in \mathbb{R}^3 onto the plane of the cross-section of the cylinder. Here, we present a proof of the existence and uniqueness of the solution for the full discrete numerical scheme. This discrete system is obtained by coupling discontinuous Galerkin (DG) numerical method applied to the RTE and finite element method (FEM) applied to the CE. Theoretical results about the stability, the convergence of the algorithm and the error estimates are presented. We previously proved the existence and uniqueness of the solution of the considered PDE system, see [1]. Moreover, a large number of numerical results has been presented in Ghattassi et al. [2]. In fact, the choice of DG methods is

Email address: mohamed.ghattassi@gmail.com (Mohamed GHATTASSI)

based on the attractive properties for the numerical approximation of hyperbolic problems, compared to both classical FEM and FVM. Indeed, in contrast with classical FEM, but together with FVM, DG methods are locally conservative concerning the state variable by construction, we refer the reader to [4] for more details.

Several numerical schemes computing an approximation of the solution of the radiation and conduction equations has been presented and analyzed in the literature. The numerical discrete ordinate method for the angular discretization of the radiative transfer equation was analyzed in Nelson et al. [5, 6]. Moreover, we find the recent work of Ya-Soung et al.[7, 8, 9, 10]. For example, in [10] the spectral collocation method is developed to study the transient heat transfer in the moving plate with temperature dependent heat generation and thermal properties. The fully implicit Euler scheme is adopted to solve the temporal discretization of dimensionless energy equation, and the spatial domain of dimensionless energy equation is discretized by Cheby-shev polynomials and Chebyshev collocation points. The convergence of spatial finite element discretization of first-order hyperbolic transport equations was studied by Lesaint and Raviart [11].

In [12], Larsen and Nelson have considered the discrete ordinate method with finite differences discretization of the radiative transfer equation with or without scattering and have given error estimates for several schemes. Results of convergence and stability for a combined spatial-angular approximation of the RTE were obtained by Pitkaranta and Scott [13] when Gauss quadrature is considered for angular discretization, and Discontinuous Galerkin DG method is used for the spatial discretization. In Scott's paper, the medium is assumed to be homogeneous, isotropic, gray and with an isotropic source term. The authors have given error estimates in L^p -norm ($1 \leq p \leq \infty$).

In [14, 15], the author has given interesting results about the convergence of spatial-angular approximations applied to the neutron equation. In [16], the authors analyzed the DG method combined with the discrete ordinate method for solving the RTE.

In the case of the CE, many recent studies have investigated the convergence and stability of the semilinear heat equation, see for instance Brezzi et al.[17] and Crysafinos et al. [18]. The convergence of the finite element method combined with the Crank-Nicolson/Newton scheme for the nonlinear parabolic equation is established in Feng et al. [19]. In the latter, the authors obtained optimal error estimates of the fully discrete Crank-Nicolson/Newton scheme of the nonlinear parabolic problem, and they illustrated the theoretical results of a numerical experiment.

This paper is devoted to the convergence of the numerical scheme for nonlinear transient radiative-conductive heat transfer system in a gray, absorbing and non-scattering two-dimensional medium. We show the existence and uniqueness of the solution of radiative-conductive heat transfer system in two-dimensional Cartesian geometry. We use the fixed point theorem to prove the well-posedness criteria of the coupled full-discrete system follows from the application of a Banach fixed-point theorem, involving only the temperature fields. Some numerical analysis arguments are used to prove separately the convergence of the RTE and the CE. An adequate norm is introduced to

prove the stability of the DG method by solving the RTE and compute an error estimate. Finally, stability condition of the numerical scheme is established.

This paper is organized as follows: In section 2, we introduce the model describing the nonlinear radiative-conductive system in two-dimensional domain. We equally give the existence and uniqueness result. We recall the full discretization of the ETR and CE in section 3. We formulate the full numerical scheme as a problem of the discrete fixed point, and we prove that it has a unique solution at each step of time in section 4. The condition guaranteeing the stability of coupled numerical scheme is also presented. Finally, in Section 5, we provide a numerical example to illustrate the theoretical results.

1. Analysis of radiative conductive heat transfer system

1.1. Model Problem

Let us consider a bounded, open, convex and connected set $\Omega \subset \mathbb{R}^2$ with C^∞ boundary. Here, Ω is a polygonal domain. Let \mathcal{D} be the unit disk and $t \in (0, \tau)$, for $\tau > 0$, $\mathcal{Q}_\tau = (0, \tau) \times \Omega$, $\mathcal{X} = \Omega \times \mathcal{D}$ and $\Sigma_\tau = (0, \tau) \times \partial\Omega$. Let \mathbf{n} be the outward unit normal to the boundary $\partial\Omega$. We denote

$$\partial\Omega_- = \{(x, \boldsymbol{\beta}) \in \partial\Omega \times \mathcal{D} \text{ such that } \boldsymbol{\beta} \cdot \mathbf{n} < 0\}.$$

Let us introduce the full system of a combined nonlinear radiation-conduction heat transfer

$$I(t, \mathbf{x}, \boldsymbol{\beta}) + \boldsymbol{\beta} \cdot \nabla_x I(t, \mathbf{x}, \boldsymbol{\beta}) = T_g^4(t, \mathbf{x}) \quad (t, \mathbf{x}, \boldsymbol{\beta}) \in (0, \tau) \times \mathcal{X} \quad (1)$$

$$\partial_t T_g(t, \mathbf{x}) - \Delta T_g(t, \mathbf{x}) + 4\pi\theta T_g^4(t, \mathbf{x}) = \theta G(t, \mathbf{x}) \quad (t, \mathbf{x}) \in \mathcal{Q}_\tau \quad (2)$$

$$T_g(t, \mathbf{x}) = g(t, \mathbf{x}) \quad (t, \mathbf{x}) \in \Sigma_\tau \quad (3)$$

$$I(t, \mathbf{x}, \boldsymbol{\beta}) = I_b(t, \mathbf{x}, \boldsymbol{\beta}) \quad (t, \mathbf{x}, \boldsymbol{\beta}) \in (0, \tau) \times \partial\Omega_- \quad (4)$$

$$T_g(0, \mathbf{x}) = T_0(\mathbf{x}) \quad \mathbf{x} \in \Omega, \quad (5)$$

where $I = I(t, \mathbf{x}, \boldsymbol{\beta})$ is the dimensionless radiation intensity, $T = T(t, \mathbf{x})$ is the dimensionless the temperature, θ is a positive dimensionless constant, T_0, I_b and g are smooth and nonnegative initial data, and

$$G(t, \mathbf{x}) = \int_{\mathcal{D}} I(t, \mathbf{x}, \boldsymbol{\beta}) \frac{2}{\sqrt{1 - |\boldsymbol{\beta}|^2}} d\boldsymbol{\beta} \quad (t, \mathbf{x}) \in \mathcal{Q}_\tau \quad (6)$$

is the incident radiation intensity.

For a fuller treatment of the dimensionless form of a combined nonlinear radiation-conduction heat transfer system in a gray, absorbing and non-scattering medium, we refer the readers to [2] and their references. Recently, the existence and uniqueness results in three-dimensional case with angular varying on the unit sphere i.e., $\boldsymbol{\beta} \in \mathcal{S}^2$ have been proposed by Ghattassi et al. in [1]. In this paper, we extend the analysis of [1] to the case of a projection of the surface

of the unit sphere in \mathbb{R}^3 onto the plane. Subsequently, the angular domain is considered as an unit disk $\beta \in \mathcal{D}$ and we will have $x \in \Omega \subset \mathbb{R}^2$.

1.2. Existence and uniqueness of solution of radiative-conductive heat transfer system

We use the following spaces as described in [1]

$$\begin{aligned} L^p(\mathcal{Q}_\tau) &:= L^p(0, \tau; L^p(\Omega)) \text{ for all } p \in [1, \infty], \\ W_p^{2,1}(\mathcal{Q}_\tau) &:= \{\phi \text{ such that } \phi, \phi_t, \phi_{x_i}, \phi_{x_i x_j} \in L^p(\mathcal{Q}_\tau)\} \forall p \in [1, \infty], \\ \mathcal{W}^2 &:= \{v \in L^2(\mathcal{X}) \text{ such that } \beta \cdot \nabla_x v \in L^2(\mathcal{X})\} \end{aligned}$$

and the following subset of $\partial\Omega \times \mathcal{D}$

$$\partial\Omega_+ = \{(x, \beta) \in \partial\Omega \times \mathcal{D} \text{ and } \beta \cdot \mathbf{n} > 0\}.$$

We denote by

$$L^2 = L^2(\mathcal{X}), \quad L_-^2 = L^2(\partial\Omega_-; -\beta \cdot \mathbf{n} \, dx d\beta)$$

and

$$L_+^2 = L^2(\partial\Omega_+; \beta \cdot \mathbf{n} \, dx d\beta),$$

the spaces of square integrable functions in \mathcal{X} , $\partial\Omega_-$ and $\partial\Omega_+$, respectively. Let us denote by \mathcal{W} the following subset of \mathcal{W}^2

$$\mathcal{W} = \{v \in \mathcal{W}^2 \text{ such that } v|_{\partial\Omega_+} \in L_+^2\},$$

a Hilbert space, for more details see [1]. The well-posedness criteria of (1)-(5) is obtained under the following assumptions

$$I_b \in H^1(0, \infty; \mathcal{W}) \cap C^2(0, \infty; C^1(\mathcal{X})) \text{ is nonnegative,}$$

$$g \in W_\infty^{2,1}((0, \infty) \times \overline{\Omega}) \cap C^2(0, \infty; C^1(\overline{\Omega})) \text{ is nonnegative,}$$

$$T_0 \text{ is nonnegative, belongs to } H^1(\Omega),$$

$$\text{There exists } \delta > 0 \text{ such that} \tag{7}$$

$$\|T_0\|_{H^1(\Omega)} \leq \delta, \quad \|g\|_{L^2(0, \tau; H^{\frac{3}{2}}(\Omega))} \leq \delta \text{ and } \|I_b\|_{H^1(0, \tau; \mathcal{W})} \leq \delta,$$

where $\delta > 0$ is sufficiently small.

$$\text{We assume that } T_0|_{\partial\Omega} = g(0, \cdot)|_{\partial\Omega}.$$

We proceed as in [1], the fixed point theorem is employed to prove the existence of solution of the nonlinear coupled radiative conductive heat transfer system (1)-(5). The existence of a solution T_g , and implicitly the existence of a solution I , of the coupled system of equations (1)-(5) is related to the existence of a solution of a fixed point problem.

We will apply the fixed point theorem to a well-chosen map \mathcal{H} . To do so, we must show that this map \mathcal{H} is completely continuous.

The map $\mathcal{H} : W_2^{2,1}(\mathcal{Q}_\tau) \longrightarrow W_2^{2,1}(\mathcal{Q}_\tau)$ is a composition of three maps

$$\mathcal{H} = \mathcal{H}_3 \circ \mathcal{H}_2 \circ \mathcal{H}_1.$$

The map $\mathcal{H}_1 : W_2^{2,1}(\mathcal{Q}_\tau) \longrightarrow L^2(\mathcal{Q}_\tau)$ is defined as follows, for $T_g \in W_2^{2,1}(\mathcal{Q}_\tau)$, $T_g^4 = \mathcal{H}_1(T_g) \in L^2(\mathcal{Q}_\tau)$. On the other hand, the map $\mathcal{H}_2 : L^2(\mathcal{Q}_\tau) \longrightarrow L^2(\mathcal{Q}_\tau)$ is defined from $L^2(\mathcal{Q}_\tau)$ to $L^2(\mathcal{Q}_\tau)$ by

$$\mathcal{H}_2(T_g^4) = \mathcal{K}[T_g]$$

where

$$G(t, \mathbf{x}) = \mathcal{K}[T_g](t, \mathbf{x}) = \int_{\mathcal{D}} \mathcal{K}_\beta T_g(t, \mathbf{x}) \frac{2}{\sqrt{1 - |\beta|^2}} d\beta \quad (t, \mathbf{x}) \in \mathcal{Q}_\tau, \quad (8)$$

where $I = \mathcal{K}_\beta T_g$ solution of the problem (1), (4). Finally, the map $\mathcal{H}_3 : L^2(\mathcal{Q}_\tau) \longrightarrow W_2^{2,1}(\mathcal{Q}_\tau)$ is defined as follows, for $G \in L^2(\mathcal{Q}_\tau)$, $\mathcal{H}_3(G) \in W_2^{2,1}(\mathcal{Q}_\tau)$ is the solution of CE (2),(3) and (5).

Recalling now under the hypothesis (7) some results established in [1].

Theorem 1.1. *Let us consider $T_g \in W_2^{2,1}(\mathcal{Q}_\tau)$. Under the assumptions (7), the problem (1), (4) has a unique nonnegative solution $I \in L^2(0, \tau; \mathcal{W})$. Moreover, there exists $C_1 = C(\tau, \Omega) > 0$ such that*

$$\|I\|_{L^2(0, \tau; \mathcal{W})} \leq C_1 \left(\|T_g\|_{W_2^{2,1}(\mathcal{Q}_\tau)}^4 + \|I_b\|_{H^1(0, \tau; \mathcal{W})} \right). \quad (9)$$

In the following proposition, we prove that $\mathcal{H}_2 \circ \mathcal{H}_1$ is a well-posed and continuous map,

Proposition 1.2. *Let $T_g \in W_2^{2,1}(\mathcal{Q}_\tau)$, the map $\mathcal{H}_2 \circ \mathcal{H}_1$ is a well-posed and continuous map from $W_2^{2,1}(\mathcal{Q}_\tau)$ to $L^2(\mathcal{Q}_\tau)$.*

Proof. Let $T_g \in W_2^{2,1}(\mathcal{Q}_\tau)$, the map \mathcal{H}_1 is a well-posed and continuous map from $W_2^{2,1}(\mathcal{Q}_\tau)$ to $L^2(\mathcal{Q}_\tau)$. The map \mathcal{H}_2 is defined from $L^2(\mathcal{Q}_\tau)$ to $L^2(\mathcal{Q}_\tau)$ by

$$\mathcal{H}_2(T_g^4) = \mathcal{K}[T_g].$$

Let $\beta \in \mathcal{D}$, $\beta \neq 0$, let $\mathcal{K}_\beta T_g$ solution of the problem (1), (4). There is no time derivative in the RTE, the intensity I varies with time because the temperature T_g does. Using simple calculation we find that

$$\mathcal{K}_\beta T_g(t, x) = \int_0^{d_\beta/|\beta|} e^{-s} T_g^4(t, x - s\beta) ds, \quad (10)$$

where $d_\beta = d(x, \beta)$ presenting the distance of x from the exterior of Ω in the direction $-\beta$,

$$d(x, \beta) = \inf\{s > 0; (x - s\beta/|\beta|) \notin \Omega\}. \quad (11)$$

T_g is constant on each vertical line, then the representation (11) is valid also for plane domain $P_r = \Omega \times \mathbb{R}$. The weight $\frac{2}{\sqrt{1-\beta^2}}$ is a consequence of the geometry. Then, from [14, Lemma1.1] and [20] it follows that \mathcal{K} is an integral operator with weakly singular kernel. Then we can deduce that \mathcal{K} is defined from $L^2(Q_\tau)$ to $L^2(0, \tau; H^1(\Omega))$ (because the operator \mathcal{K} is implicitly dependent on time). Hence $\mathcal{K} : L^2(Q_\tau) \rightarrow L^2(Q_\tau)$ is compact.

Finally, it follows that $\mathcal{H}_2 \circ \mathcal{H}_1$ is a continuous map from $W_2^{2,1}(Q_\tau)$ to $L^2(Q_\tau)$.

Moreover, \mathcal{H}_2 is a compact map then there exists $C_2 = C(\tau, \Omega) > 0$ such that

$$\|G\|_{L^2(Q_\tau)} \leq C_2 \left(\|T_g\|_{W_2^{2,1}(Q_\tau)}^4 + \|I_b\|_{H^1(0,\tau;\mathbf{W})} \right). \quad (12)$$

This finishes the proof. \square

Now we introduce some properties of the map \mathcal{H}_3 for more details see [1].

Proposition 1.3. *Let $\tau > 0$, $G \in L^2(Q_\tau)$. Under the assumptions (7), the problem (2),(3),(5) has a nonnegative solution $T_g \in W_2^{2,1}(Q_\tau)$. Moreover, there exist $C_3 = C(\Omega, \tau, \theta) > 0$ such that*

$$\|T_g\|_{W_2^{2,1}(Q_\tau)} \leq C_3 \left(\|G\|_{L^2(Q_\tau)} + \|T_0\|_{H^1(\Omega)} + \|g\|_{L^2(0,\tau;H^{\frac{3}{2}}(\Omega))} \right) \quad (13)$$

and \mathcal{H}_3 is a continuous map from $L^2(Q_\tau)$ to $W_2^{2,1}(Q_\tau)$.

The main result of this section is the following theorem.

Theorem 1.4. *Assume that the data verifies (7). For all $\tau > 0$, there exists $\delta = \delta(\Omega, \tau, \theta) > 0$ such that*

$$\|T_0\|_{H^1(\Omega)} \leq \delta, \quad \|g\|_{L^2(0,\tau;H^{\frac{3}{2}}(\Omega))} \leq \delta \text{ and } \|I_b\|_{H^1(0,\tau;\mathbf{W})} \leq \delta.$$

Then the system of equations (15)-(19) has a unique nonnegative solution (T_g, I) such that $T_g \in W_2^{2,1}(Q_\tau)$ and $I \in L^2(0, \tau; \mathbf{W})$. Moreover, there exists $C(\Omega, \tau, \theta) > 0$ such that

$$\|T_g\|_{W_2^{2,1}(Q_\tau)} \leq C(\Omega, \tau, \theta) \left(\|I_b\|_{H^1(0,\tau;\mathbf{W})} + \|T_0\|_{H^1(\Omega)} + \|g\|_{L^2(0,\tau;H^{\frac{3}{2}}(\Omega))} \right). \quad (14)$$

Proof. For the proof see [1]. \square

Remark 1.5. • *The results of this section can also be extended to nonhomogenous Neumann boundary conditions by a lifting trace argument, provided that the boundary value is regular enough.*

- *We extend the analysis to the case of a projection of the surface of the unit sphere in \mathbb{R}^3 onto the plane, i.e., $\beta \in \mathcal{D}$. The compactness of the operator \mathcal{K} has been used to prove the continuity of the map \mathcal{H}_2 .*

2. Numerical approximation of radiative and conductive heat transfer system

For numerical analysis purpose the nonhomogeneous Dirichlet is most easily handled by subtracting out the boundary values by extending them to a function defined in all $[0, \tau] \times \overline{\Omega}$ and changing the depend variable. If the boundary values for T_g are given by $g(t, x)$, consider

$$T_g(t, x) - g(t, x) \in H_0^1(\Omega).$$

We will approximate T_g by approximating $T = T_g - g$. Then, using the previous techniques (1)-(5) becomes

$$I(t, \mathbf{x}, \boldsymbol{\beta}) + \boldsymbol{\beta} \cdot \nabla_{\mathbf{x}} I(t, \mathbf{x}, \boldsymbol{\beta}) = Q[T](t, \mathbf{x}) \quad (t, \mathbf{x}, \boldsymbol{\beta}) \in (0, \tau) \times \mathcal{X} \quad (15)$$

$$\partial_t T(t, \mathbf{x}) - \Delta T(t, \mathbf{x}) + 4\pi\theta Q[T](t, \mathbf{x}) = \theta G(t, \mathbf{x}) \quad (t, \mathbf{x}) \in \mathcal{Q}_\tau \quad (16)$$

$$T(t, \mathbf{x}) = 0 \quad (t, \mathbf{x}) \in \Sigma_\tau \quad (17)$$

$$I(t, \mathbf{x}, \boldsymbol{\beta}) = I_b(t, \mathbf{x}, \boldsymbol{\beta}) \quad (t, \mathbf{x}, \boldsymbol{\beta}) \in (0, \tau) \times \partial\Omega_- \quad (18)$$

$$T(0, \mathbf{x}) = T_0(\mathbf{x}) \quad \mathbf{x} \in \Omega \quad (19)$$

where

$$Q[T] \equiv (T + g)^4.$$

The system (15)-(19) will be used throughout the paper to analyze the numerical scheme.

2.1. Numerical discretization of the radiative transfer equation

2.1.1. Angular discretization

In order to define our discrete-ordinate DG methods for the problem (15),(18), we approximate the integration term G appearing in (16) by certain quadrature. The numerical quadrature is given in the following form

$$\int_{\mathcal{D}} I(\boldsymbol{\beta}) d\boldsymbol{\beta} = \sum_{l=1}^{N_\beta} I(\boldsymbol{\beta}_l) w_l \quad w_l > 0, \boldsymbol{\beta}_l \in \mathcal{D}, l \in \{1, \dots, N_\beta\}$$

where I is a continuous function over the unit sphere \mathcal{D} . A popular choice of quadratures in relevant engineering literature is the S_N family that has prescribed geometric symmetry for the set of the quadrature nodes on the unit sphere, and we refer to [21] for details along this line and for error analysis of this methods. The S_N method consists in computing the radiation intensity $I(t, \mathbf{x}, \boldsymbol{\beta})$ in a finite number of directions $\boldsymbol{\beta}_l, l \in \{1, \dots, N_\beta\}$. We obtain a discrete radiation intensity $(I^1(t, \mathbf{x}), I^2(t, \mathbf{x}), \dots, I^{N_\beta}(t, \mathbf{x}))$; where $I^l(t, \mathbf{x}) = I(t, \mathbf{x}, \boldsymbol{\beta}_l)$ for all $l \in \{1, \dots, N_\beta\}$.

The discrete radiation intensity I^l is the solution of a N_β system of partial differential equations over Ω :

$$\begin{cases} \boldsymbol{\beta}_l \cdot \nabla I^l(t, \mathbf{x}) + I^l(t, \mathbf{x}) = T^4(t, \mathbf{x}), & (t, \mathbf{x}) \in (0, \tau) \times \Omega, \\ I^l(t, \mathbf{x}) = I_b^l(t, \mathbf{x}), & (t, \mathbf{x}) \in (0, \tau) \times \partial\Omega_-^l, \end{cases} \quad (20)$$

where

$$\partial\Omega_-^l = \{\mathbf{x} \in \partial\Omega \text{ such that } \boldsymbol{\beta}_l \cdot \mathbf{n} < 0\}$$

and $h^l(t, \mathbf{x}) = h(t, \mathbf{x}, \boldsymbol{\beta}_l)$ is the radiative boundary conditions for all $l \in \{1, \dots, N_\beta\}$.

The quadrature integrates exactly all spherical polynomials of total degree no more than m and does not integrate exactly some spherical polynomial of total degree $m + 1$, see [22, 23, 16, 3] given in \mathcal{S}^2 .

The following theorem gives the error estimate of the angular approximation.

Theorem 2.1. *Let I be a function define on \mathcal{D} , and let $\{\beta_l\}_{l=1}^{N_\beta}$ and $\{w_l\}_{l=1}^{N_\beta}$ be a set of nodes and weights, respectively, such that $w_l > 0$ for all $1 \leq l \leq N_\beta$*

$$\int_{\mathcal{D}} p(\beta) d\beta = \sum_{l=1}^{N_\beta} w_l p(\beta_l), \quad (21)$$

for all polynomials p of degree no more than m and if $I \in H^r(\mathcal{D})$, $r > 1$ then

$$\left| \sum_{l=1}^{N_\beta} w_l I(\beta_l) - \int_{\mathcal{D}} I(\beta) d\beta \right| \leq C_r m^{-r} \|I\|_{H^r(\mathcal{D})}, \quad (22)$$

where C_r is a positive constant depending only on r .

2.1.2. Discontinuous Galerkin method for solving the RTE

Now, we proceed with the spatial discretization of the S_N transport equation (20) using the DG method. We consider a triangulation \mathcal{T}_h of Ω described by a mesh size h such that

$$\overline{\Omega} = \bigcup_{K \in \mathcal{T}_h} K,$$

- Each K is a triangle with nonempty internal;
- $\overset{\circ}{K}_1 \cap \overset{\circ}{K}_2 = \emptyset$ for each distinct $K_1, K_2 \in \mathcal{T}_h$;
- $F = K_1 \cap K_2 \neq \emptyset$ then F is a common face of K_1 and K_2 ;
- Interfaces are collected in the set \mathcal{F}_h^{in} and boundary faces are collected in the set \mathcal{F}_h^b . Henceforth, we set

$$\mathcal{F}_h = \mathcal{F}_h^{in} \cup \mathcal{F}_h^b.$$

Moreover, for any mesh element $K \in \mathcal{T}_h$, the set

$$\mathcal{F}_K = \{F \in \mathcal{F}_h | F \in \partial K\},$$

collects the mesh faces composing the boundary of K .

- $N_{\mathcal{T}}$ denotes the number of nodes of mesh \mathcal{T}_h , $N_{\partial\Omega}$ the number of nodes in $\partial\Omega$ and N_b the number of nodes in $\partial\Omega_-$.

Now, an approximation space $V_h \subset H^1(\Omega)$ is introduced such that

$$V_h = \{I_h \in H^1(\Omega) / \forall K \in \mathcal{T}_h, I_{h|_K} \in \mathbb{P}^p(K)\}, \quad (23)$$

where $\mathbb{P}^p(K)$ denotes the set of polynomial defined in K of degree less than or equal to p .

This gives the following properties of the jump of I^l across interfaces, for all $F \in \mathcal{F}_h^{in}$

$$(\boldsymbol{\beta}_l \cdot \mathbf{n}_F) \llbracket I^l \rrbracket(\mathbf{x}) = 0 \quad \text{for } \mathbf{x} \in F \quad (24)$$

where \mathbf{n}_F is the outward unit normal to F at \mathbf{x} , see [4, Lemma 2.14].

Define

$$\mathbb{V}_h = \{V_h\}_{l=1}^{N_\beta}$$

and denote a generic element in \mathbb{V}_h as $I_h(t, \cdot) = \{I_h^l(t, \cdot)\}_{l=1}^{N_\beta}$. Due to the discontinuous nature of the spatial approximation, functions $I_h^l \in V_h$ is double-valued on interior faces. Consider an interior face $F \in \mathcal{F}_h^{in}$ separating two mesh cells, K_1 and K_2 . The mean value and jump of a function $I_h^l(t, \cdot) \in V_h$ are defined as follows:

$$\{\{I_h^l(t, \cdot)\}\} = \frac{1}{2}(I_1^l(t, \cdot) + I_2^l(t, \cdot)), \quad \llbracket I_h^l(t, \cdot) \rrbracket = (I_1^l(t, \cdot) - I_2^l(t, \cdot)),$$

for all $t \in (0, \tau)$, where $I_1^l(t, \cdot) = I_h^l(t, \cdot)|_{K_1}$ and $I_2^l(t, \cdot) = I_h^l(t, \cdot)|_{K_2}$ are the restrictions of $I_h^l(t, \cdot)$ on the mesh cells K_1 and K_2 , respectively.

The DG formulation is obtained by multiplying the S_N equation for the direction $\boldsymbol{\beta}_l$ with the test function $w_h \in \mathbb{V}_h$ and applying the upwind numerical fluxes $\hat{\mathcal{F}}(\mathbf{x})$ to approximate the quantity $(\boldsymbol{\beta}_l \cdot \mathbf{n})I^l(t, \cdot)$ on the elements boundary ∂K ;

$$\int_K I_h^l(t, \cdot) w_h - (\boldsymbol{\beta}_l \cdot \nabla_h w_h) I_h^l(t, \cdot) + \int_{\partial K} \hat{\mathcal{F}}(\mathbf{x}) w_h = \int_\Omega T_h^A(t, \cdot) w_h, \quad \forall t \in (0, \tau).$$

We extend the boundary datum I_b to $\partial\Omega$ by setting it to zero outside $\partial\Omega_-$ and we assume that $h \in H^1(0, \tau; \mathcal{W})$. The upwind numerical flux $\hat{\mathcal{F}}(\mathbf{x})$ at the mesh interface F from K_1 to K_2 is given by

$$\hat{\mathcal{F}}(\mathbf{x}) = \begin{cases} \boldsymbol{\beta}_l \cdot \mathbf{n}_F \{\{I^l(t, \mathbf{x})\}\} + \frac{1}{2} |\boldsymbol{\beta}_l \cdot \mathbf{n}_F| \llbracket I^l(t, \mathbf{x}) \rrbracket, & \forall F \in \mathcal{F}_h^{in} \\ (\boldsymbol{\beta}_l \cdot \mathbf{n})^\oplus I_h^l(t, \cdot) - (\boldsymbol{\beta}_l \cdot \mathbf{n})^\ominus I_b^l(t, \cdot), & \forall F \in \mathcal{F}_h^b \end{cases} \quad \forall t \in (0, \tau).$$

Summing over all cells, integrating by parts a second time and separating volume and interface terms, we obtain a

global formulation. Upon introducing the bilinear form

$$\begin{aligned}
a_h^{up}(I_h(t, \cdot), w_h) &= \sum_{l=1}^{N_\beta} w_l \sum_{K \in \mathcal{T}_h} \left[\int_K I_h^l(t, \cdot) w_h^l d\mathbf{x} - \int_K I_h^l(t, \cdot) (\boldsymbol{\beta}_l \cdot \nabla w_h^l) d\mathbf{x} \right] \\
&\quad + \int_{\partial\Omega} (\boldsymbol{\beta}_l \cdot \mathbf{n})^\oplus I_h^l(t, \cdot) w_h^l d\Gamma(\mathbf{x}) \\
&\quad + \sum_{F \in \mathcal{F}_h^{in}} \int_F (\boldsymbol{\beta}_l \cdot \mathbf{n}_F) \llbracket I_h^l(t, \cdot) \rrbracket \{\{w_h^l\}\} d\Gamma(\mathbf{x}) \\
&\quad + \sum_{F \in \mathcal{F}_h^{in}} \int_F \frac{1}{2} |\boldsymbol{\beta}_l \cdot \mathbf{n}_F| \llbracket I_h^l(t, \cdot) \rrbracket \llbracket w_h^l \rrbracket d\Gamma(\mathbf{x}),
\end{aligned}$$

for all $(t, w_h) \in (0, \tau) \times \mathbb{V}_h$, where for a real number x ; we define its nonnegative and negative parts, respectively, by $x^\oplus := \frac{1}{2}(|x| + x)$, $x^\ominus := \frac{1}{2}(|x| - x)$. By definition, the both quantities are nonnegative. The following linear form $l_h : \mathbb{V}_h \rightarrow \mathbb{R}$ is defined, for all $(t, w_h) \in (0, \tau) \times \mathbb{V}_h$ by

$$l(w_h) = \sum_{l=1}^{N_\beta} w_l \left[\int_\Omega Q[T_h] w_h^l d\mathbf{x} + \int_{\partial\Omega} (\boldsymbol{\beta}_l \cdot \mathbf{n})^\ominus I_b^l w_h^l d\mathbf{x} \right]$$

where T_h is the approximate solution of T using finite elements method.

The discrete ordinate DG problem is written as :

$$\begin{aligned}
&\text{Find } \{I_h\}(t) \in \mathbb{V}_h \text{ such as} \\
&a_h^{up}(\{I_h\}(t), w_h) = l_h(w_h) \text{ for all } (t, w_h) \in (0, \tau) \times \mathbb{V}_h.
\end{aligned} \tag{25}$$

By discretizing the time interval $[0; \tau]$ using a time step $\Delta t > 0$. We obtain a discretization $t_n = n\Delta t$ where $n \in \llbracket 0, \dots, N_\tau \rrbracket$. The full discrete system (25) is given by

$$\begin{aligned}
&\text{Find } \{I_h\}^n \in \mathbb{V}_h \text{ such as} \\
&a_h^{up}(\{I_h\}^n, w_h) = l_h(w_h) \text{ for all } (n, w_h) \in \llbracket 0, \dots, N_\tau \rrbracket \times \mathbb{V}_h.
\end{aligned} \tag{26}$$

where $\{I_h\}^n = \{I_h\}(t_n)$ for all $n \in \llbracket 0, \dots, N_\tau \rrbracket$.

2.1.3. Consistency, discrete coercivity and convergence

We can now summarize the properties of the discrete bilinear form a_h^{up} establish so far. We first examine the consistency and discrete coercivity of the DG scheme (25) by introducing the following norm $\|\cdot\|_h$ definite in \mathbb{V}_h by

$$\|I\|_h^2 = \sum_{l=1}^{N_\beta} w_l \left[\|I^l\|_{L^2(\Omega)}^2 + \int_{\partial\Omega} \frac{1}{2} |\boldsymbol{\beta}_l \cdot \mathbf{n}| I^l{}^2 d\Gamma(\mathbf{x}) + \sum_{F \in \mathcal{F}_h^{in}} \int_F \frac{1}{2} |\boldsymbol{\beta}_l \cdot \mathbf{n}_F| \llbracket I^l \rrbracket^2 d\Gamma(\mathbf{x}) \right]$$

for all $\{I\} \in \mathbb{V}_h$, see [4, Section 2.3]. Using this definition, we can derived the following lemma

Lemma 2.2. *The DG scheme defined by (25) satisfies the following properties*

- Consistency, namely for the exact solution $\{I\} \in \{\mathcal{V}_*\}$

$$a_h^{up}(\{I\}(t_n), \{w_h\}) = \sum_{l=1}^{N_\beta} w_l \left[\int_{\Omega} Q[T](t_n) w_h^l dx + \int_{\partial\Omega} (\boldsymbol{\beta}_l \cdot \mathbf{n})^\ominus h^l w_h^l dx \right]$$

for all $(n, \{w_h\}) \in \llbracket 0, \dots, N_\tau \rrbracket \times \mathbb{V}_h$.

- Coercivity on \mathbb{V}_h with respect to the $\llbracket \{I\} \rrbracket_h$ namely

$$a_h^{up}(\{I_h\}(t_n), \{I_h\}(t_n)) = \llbracket \{I_h\}(t_n) \rrbracket_h^2 \quad (27)$$

for all $(n, \{I_h\}(t_n)) \in \llbracket 0, \dots, N_\tau \rrbracket \times \mathbb{V}_h$.

Proof. The consistency of a_h^{up} results from $(\boldsymbol{\beta}_l \cdot \mathbf{n}_F) \llbracket I^l(t, \cdot) \rrbracket = 0$ for all $F \in \mathcal{F}_h^{in}$ owing (24). Concerning coercivity, let $n \in \llbracket 0, \dots, N_\tau \rrbracket$, $\{I_h\}(t_n) \in \mathbb{V}_h$, by definition of $a_h^{up}(\cdot, \cdot)$, we have

$$\begin{aligned} a_h^{up}(\{I_h\}(t_n), \{I_h\}(t_n)) &= \sum_{l=1}^{N_\beta} w_l \sum_{K \in \mathcal{T}_h} \left(\int_K (I_h^l(t_n, \mathbf{x}))^2 dx - \int_K I_h^l (\boldsymbol{\beta}_l \cdot \nabla I_h^l(t_n, \mathbf{x})) dx \right) \\ &\quad + \int_{\partial\Omega} (\boldsymbol{\beta}_l \cdot \mathbf{n})^\ominus (I_h^l(t_n, \mathbf{x}))^2 d\Gamma(\mathbf{x}) \\ &\quad + \sum_{F \in \mathcal{F}_h^{in}} \int_F \frac{1}{2} |\boldsymbol{\beta}_l \cdot \mathbf{n}_F| (\llbracket I_h^l(t_n, \mathbf{x}) \rrbracket)^2 d\Gamma(\mathbf{x}) \\ &\quad + \sum_{F \in \mathcal{F}_h^{in}} \int_F (\boldsymbol{\beta}_l \cdot \mathbf{n}_F) \llbracket I_h^l(t_n, \mathbf{x}) \rrbracket \{I_h^l(t_n, \mathbf{x})\} d\Gamma(\mathbf{x}). \end{aligned}$$

Using integration by parts, we obtain

$$\begin{aligned} a_h^{up}(\{I_h\}(t_n), \{I_h\}(t_n)) &= \sum_{l=1}^{N_\beta} w_l \sum_{K \in \mathcal{T}_h} \left[\int_K (I_h^l(t_n, \mathbf{x}))^2 dx - \frac{1}{2} \int_{\partial K} (\boldsymbol{\beta}_l \cdot \mathbf{n}_K) (I_h^l(t_n, \mathbf{x}))^2 dx \right] \\ &\quad + \int_{\partial\Omega} (\boldsymbol{\beta}_l \cdot \mathbf{n})^\ominus (I_h^l(t_n, \mathbf{x}))^2 d\Gamma(\mathbf{x}) \\ &\quad + \sum_{F \in \mathcal{F}_h^{in}} \int_F \frac{1}{2} |\boldsymbol{\beta}_l \cdot \mathbf{n}_F| (\llbracket I_h^l(t_n, \mathbf{x}) \rrbracket)^2 d\Gamma(\mathbf{x}) \\ &\quad + \sum_{F \in \mathcal{F}_h^{in}} \int_F (\boldsymbol{\beta}_l \cdot \mathbf{n}_F) \llbracket I_h^l(t_n, \mathbf{x}) \rrbracket \{I_h^l(t_n, \mathbf{x})\} d\Gamma(\mathbf{x}). \end{aligned}$$

The second term on the right hand side can be formulated. Indeed, the continuity of $\boldsymbol{\beta}_l$ across interfaces leads to

$$\begin{aligned} \sum_{K \in \mathcal{K}_h} \int_{\partial K} \frac{1}{2} (\boldsymbol{\beta}_l \cdot \mathbf{n}_K) (I_h^l(t_n, \mathbf{x}))^2 &= \sum_{F \in \mathcal{F}_h^{in}} \int_F \frac{1}{2} (\boldsymbol{\beta}_l \cdot \mathbf{n}_F) \llbracket I_h^l(t_n, \mathbf{x}) \rrbracket^2 \\ &\quad + \sum_{F \in \mathcal{F}_h^b} \int_F \frac{1}{2} (\boldsymbol{\beta}_l \cdot \mathbf{n}_F) I_h^l{}^2(t_n, \mathbf{x}), \end{aligned}$$

for all $F \in \mathcal{F}_h^{in}$ with $F = \partial K_1 \cap \partial K_2$, $I_i = I_{h|_{K_i}}^l$, $i \in \{1, 2\}$. Then, we have

$$\frac{1}{2} \llbracket I_h^l{}^2 \rrbracket = \frac{1}{2} (I_1^2 - I_2^2) = \frac{1}{2} (I_1 - I_2)(I_1 + I_2) = \llbracket I_h^l \rrbracket \{I_h^l\}.$$

Hence, it follows that

$$a_h^{up}(\{I_h\}(t_n), \{I_h\}(t_n)) = \sum_{l=1}^{N_\beta} w_l \left\| I_h^l(t_n, \cdot) \right\|_{L^2(\Omega)}^2 + \frac{1}{2} \int_{\partial\Omega} |\beta_l \cdot \mathbf{n}| (I_h^l(t_n, \mathbf{x}))^2 d\Gamma(\mathbf{x}) \\ + \sum_{F \in \mathcal{F}_h^{\text{in}}} \int_F \frac{1}{2} |\beta_l \cdot \mathbf{n}_F| \left\| I_h^l(t_n, \mathbf{x}) \right\|^2 d\Gamma(\mathbf{x}).$$

Consequently,

$$a_h^{up}(\{I_h\}(t_n), \{I_h\}(t_n)) = \left\| \{I_h\}(t_n) \right\|_h^2$$

□

Remark 2.3. l_h is a linear and continuous map in \mathbb{V}_h to \mathbb{R} , using lemma 2.2 it follows that (25) has a unique solution in \mathbb{V}_h .

2.2. Numerical approximation of the conductive equation

In this paragraph we introduce the numerical method to solve the following conductive equation.

$$\begin{cases} \partial_t T(t, \mathbf{x}) - \Delta T(t, \mathbf{x}) + 4\pi\theta Q[T](t, \mathbf{x}) = \theta G(t, \mathbf{x}) & (t, \mathbf{x}) \in \mathcal{Q}_\tau \\ T(t, \mathbf{x}) = 0 & (t, \mathbf{x}) \in \Sigma_\tau \\ T(0, \mathbf{x}) = T_0(\mathbf{x}) & (t, \mathbf{x}) \in \Omega. \end{cases} \quad (28)$$

In fact, we consider a classical numerical method; the Crank-Nicolson implicit scheme for temporal discretization and finite element method for the space approximation of the solution in each time step. We assume that $G \in L^2(\mathcal{Q}_\tau)$. The finite element formulation is based on the Galerkin approximation of T in the subspace $W_h \subset H_0^1(\Omega)$ given by

$$W_h = \{v_h \in C^0(\Omega) \cap H_0^1(\Omega) / \forall K \in \mathcal{T}_h, v_h|_K \in \mathbb{P}^p(K)\}. \quad (29)$$

In the proposed formulation, at each time step n we seek $T_h^n \in W_h$ the solution of the following equation:

$$\left(\frac{T_h^{n+1} - T_h^n}{\Delta t}, v_h \right) + a \left(\frac{T_h^{n+1} + T_h^n}{2}, v_h \right) \\ + 4\pi\theta \left(\frac{Q[T_h^{n+1}] + Q[T_h^n]}{2}, v_h \right) = \theta \left(\frac{G^{n+1} + G^n}{2}, v_h \right), \quad \forall v_h \in W_h. \quad (30)$$

where

$$G_h^{n+1} = \sum_{l=1}^{N_\beta} w_l I_h^{l,n+1},$$

and $\{I_h^l\}^n$ is the solution of the RTE.

The function $a(T_h^n, v_h)$ is the well known coercive bilinear form:

$$a(T, v) := \int_{\Omega} \nabla T \cdot \nabla v dx, \quad \forall T, v \in H_0^1(\Omega).$$

For more details about the consistency of the numerical scheme for semilinear parabolic equation we refer the reader to [18] and their references. A deeper discussion of the analysis of Crank-Nicolson-Galerkin approximation to approach the solution of nonlinear parabolic problems is presented in [24].

2.3. Numerical Scheme for the coupled system

In the previous sections, we have described the numerical method considered to solve the RTE and CE. In this section, we introduce the algorithm that we propose to compute a numerical approximation of the solution of the coupled system in the domain Ω during a period $(0, \tau]$ when we give the initial temperature T_0 in Ω and boundary conditions.

The numerical scheme to compute an approximation of the solution of the system (15)-(19) is inspired by the method that we have used to prove the existence and uniqueness of a solution of the radiative-conductive heat transfer system. After a classical temporal discretization, we consider at each time step a fixed point method.

Given the final time τ and $N_\tau \in \mathbb{N}$, let Δt be a time step verifying $\tau = N_\tau \Delta t$. The index n will denote the time step and the index k the fixed point algorithm step. Let denote T_{0h} the projection in W_h of the initial data T_0 . The numerical solution $(\{I_h^l\}^n, T_h^n)$ of the system (15)-(19) at time t^n for $n = 1, \dots, N_\tau$ is obtained using the following algorithm:

- For $n = 0, \dots, N_\tau - 1$

$$T_h^{n+1(0)} = T_h^n$$

- For $k = 0, \dots$, until convergence of the fixed point loop

- a) Solve the RTE

$$a_h^{up}(\{I_h^l\}^{n+1(k+1)}, \{I_h^l\}^{n+1(k+1)}) = I_h(\{I_h^l\}^{n+1(k)}) \quad (31)$$

- b) Compute

$$G_h^{n+1(k+1)} = \sum_{l=1}^{N_\beta} w_l I_h^{l, n+1(k+1)},$$

- c) Solve

$$\begin{aligned} & \left(\frac{T_h^{n+1(k+1)} - T_h^n}{\Delta t}, v_h \right) + a \left(\frac{T_h^{n+1(k+1)} + T_h^n}{2}, v_h \right) \\ & + 4\pi\theta \left(\frac{Q[T_h^{n+1(k+1)}] + Q[T_h^n]}{2}, v_h \right) \\ & = \theta \left(\frac{G_h^{n+1(k)} + G_h^n}{2}, v_h \right) \quad \forall v_h \in W_h, \end{aligned} \quad (32)$$

- End of the fixed point loop.

- End of the temporal loop.

The nonlinear equation (32) is solved using Newton's method. In the next section, we show the proof of the existence and uniqueness of the solution of the full discrete system using a fixed point argument. Moreover, we give a convergence proof, error estimates and stability conditions.

3. Numerical analysis for the full discrete system

3.1. Existence and uniqueness of the solution for full discrete system

The idea of this section is to apply the Banach fixed point theorem to prove the existence and uniqueness of the solution of the full numerical scheme describing the nonlinear coupled radiative conductive heat transfer system for the discrete time t_n for all $n \in \llbracket 0, \dots, N_\tau \rrbracket$. The proof is based on the approximate temperature T_h^n .

Let introduce the following norm

$$\begin{aligned} \|g\|_{\infty,h} &= \sup_{n \in \llbracket 0, \dots, N_\tau \rrbracket} \|g^n\|_{W_h} \quad \forall g \in L^\infty(\mathbb{R}^{N_\tau}; W_h), \\ \|I_b\|_{\beta, \infty, h} &= \sup_{(l,n) \in \llbracket 0, \dots, N_\beta \rrbracket \times \llbracket 0, \dots, N_\tau \rrbracket} \|I_b^{l,n}\|_{V_h} \quad \forall g \in L^\infty(\mathbb{R}^{N_\tau} \times \mathbb{R}^{N_\beta}; V_h), \end{aligned}$$

in $L^\infty(\mathbb{R}^{N_\tau}; W_h)$ and $L^\infty(\mathbb{R}^{N_\tau} \times \mathbb{R}^{N_\beta}; V_h)$, respectively. Moreover, there exists $\delta > 0$ such that

$$\|T_0\|_{W_h} \leq \delta, \quad \|g\|_{\infty,h} \leq \delta \text{ and } \|I_b\|_{\beta, \infty, h} \leq \delta, \quad (33)$$

where $\delta > 0$ is sufficiently small.

Our goal is to show that $\tilde{\mathcal{H}}_h^n$ is a well-posed, continuous map and has a unique fixed-point. We express $\tilde{\mathcal{H}}_h^n$ with the composition of two nonlinear maps

$$\tilde{\mathcal{H}}_h^n = \tilde{\mathcal{H}}_{2h}^n \circ \tilde{\mathcal{H}}_{1h}^n.$$

We define the map $\tilde{\mathcal{H}}_{1h}^n : W_h \rightarrow V_h$ where for all $T_h^n \in W_h$, $\tilde{\mathcal{H}}_{1h}^n(T_h^n) \in V_h$ is the solution of the RTE (31). Finally, we define the map $\tilde{\mathcal{H}}_{2h}^n : V_h \rightarrow W_h$ such that for all $\{I_h^l\}^n \in V_h$, $\tilde{\mathcal{H}}_{2h}^n(\{I_h^l\}^n) \in W_h$ is the solution of the equation (32).

Lemma 3.1. *Let $n \in \llbracket 0, \dots, N_\tau \rrbracket$, $T_h^n \in W_h$. $\tilde{\mathcal{H}}_{1h}^n$ is a well-posed and continuous map from W_h to V_h .*

Proof. Let $n \in \llbracket 0, \dots, N_\tau \rrbracket$, $T_h^n \in W_h$, from (26)-(27) it follows that

$$\begin{aligned} \|\{I_h\}^n\|_h^2 &= a_h^{up}(\{I_h\}(t_n), \{I_h\}(t_n)) \\ &= \sum_{l=1}^{N_\beta} w_l \left[\int_{\Omega} Q[T_h^n] I_h^{l,n} dx + \int_{\partial\Omega} (\beta_l \cdot \mathbf{n})^\ominus I_b^{l,n} I_h^{l,n} dx \right], \end{aligned}$$

then using Young inequality There exists $C = C(\Omega) > 0$

$$\|\{I_h\}^n\|_h \leq C \left(\|T_h^n\|_{W_h}^4 + \|g\|_{\infty,h}^4 + \|I_b\|_{\beta, \infty, h} \right). \quad (34)$$

Hence $\tilde{\mathcal{H}}_{1h}^n$ is a well-posed continuous map from W_h to V_h . \square

Lemma 3.2. Let $n \in \llbracket 0, \dots, N_\tau \rrbracket$, $T_h^n \in W_h$ and $\{I_h^l\}^n \in \mathbb{V}_h$, $\tilde{\mathcal{H}}_{2h}^n$ is a well-posed and continuous map from \mathbb{V}_h to W_h .

Proof. Let $n \in \llbracket 0, \dots, N_\tau - 1 \rrbracket$. We take $v_h = T_h^{n+1} + T_h^n$ in (32). Using the non-negativity of the initial data and the Young's inequality, it follows that for all $\epsilon > 0$ we have

$$\begin{aligned} \|T_h^{n+1}\|_{L^2(\Omega)}^2 + \frac{\Delta t}{2} \|\nabla(T_h^{n+1} + T_h^n)\|_{L^2(\Omega)}^2 &\leq \Delta t \frac{\theta}{4\epsilon} \|G_h^{n+1} + G_h^n\|_{L^2(\Omega)}^2 \\ &+ \|T_h^n\|_{L^2(\Omega)}^2 + \Delta t \theta \frac{\epsilon}{4} \|T_h^{n+1} + T_h^n\|_{L^2(\Omega)}^2. \end{aligned}$$

There exists $C(\Omega) > 0$ such that

$$\begin{aligned} \|T_h^{n+1}\|_{L^2(\Omega)}^2 + \frac{\Delta t}{2} \|T_h^{n+1} + T_h^n\|_{H_0^1(\Omega)}^2 &\leq \Delta t \frac{\theta}{4\epsilon} \|G_h^{n+1} + G_h^n\|_{L^2(\Omega)}^2 \\ &+ \|T_h^n\|_{L^2(\Omega)}^2 + \Delta t \theta \frac{\epsilon}{4} C(\Omega) \|T_h^{n+1} + T_h^n\|_{H_0^1(\Omega)}^2. \end{aligned}$$

Choosing $\epsilon = \frac{2}{\theta C(\Omega)}$, we obtain

$$\|T_h^{n+1}\|_{L^2(\Omega)}^2 \leq \Delta t \frac{\theta^2 C(\Omega)}{8} \|G_h^{n+1} + G_h^n\|_{L^2(\Omega)}^2 + \|T_h^n\|_{L^2(\Omega)}^2.$$

then

$$\|T_h^{n+1}\|_{L^2(\Omega)}^2 \leq \pi \Delta t \frac{\theta^2 C(\Omega)}{2} \|\{I_h\}^{n+1} + \{I_h\}^n\|_h^2 + \|T_h^n\|_{L^2(\Omega)}^2. \quad (35)$$

Finally, using the fact that $T_h^n \in W_h$, we have $T_h^{n+1} \in W_h$. Hence $\tilde{\mathcal{H}}_{2h}^n$ is a well-posed and continuous map. This finishes the proof. \square

Now, we prove the existence and uniqueness of the solution for the system (31)-(32) using the Banach fixed-point theorem.

Theorem 3.3. Let $n \in \llbracket 0, \dots, N_\tau \rrbracket$. Under the assumptions (33), the system (31)-(32) has a unique solution $(T_h^n, \{I_h\}^n) \in W_h \times \mathbb{V}_h$.

Proof. Let $n \in \llbracket 0, \dots, N_\tau \rrbracket$. From Lemma 3.1 and Lemma 3.2, we conclude that $\tilde{\mathcal{H}}_h^n = \tilde{\mathcal{H}}_{2h}^n \circ \tilde{\mathcal{H}}_{1h}^n$ is a well-posed map because it is composed of two well-posed maps.

From (34) and (35), we conclude that there exists $C = C(\Delta t, \Omega) > 0$ such that

$$\|T_h^{n+1}\|_{W_h} \leq C \left(\|T_h^{n+1}\|_{W_h}^4 + \|g\|_{\infty, h}^4 + \|I_b\|_{\beta, \infty, h} + \|T_{0h}\|_{W_h} \right). \quad (36)$$

Let us consider $(T_{1h}^{n+1}, \{I_{1h}^l\}^{n+1})$ and $(T_{2h}^{n+1}, \{I_{2h}^l\}^{n+1})$ solutions of the full discrete numerical system describing the nonlinear radiative conductive heat transfer. Hence

$$\begin{aligned} (T_{1h}^{n+1} - T_{2h}^{n+1}, v_h) + \frac{\Delta t}{2} a(T_{1h}^{n+1} - T_{2h}^{n+1}, v_h) \\ + 2\pi\theta\Delta t (Q[T_{1h}^{n+1}] - Q[T_{2h}^{n+1}], v_h) = \theta \frac{\Delta t}{2} (G_{1h}^{n+1} - G_{2h}^{n+1}, v_h). \end{aligned} \quad (37)$$

Let us assume $v_h = T_{1h}^{n+1} - T_{2h}^{n+1}$ and using the fact that

$$\left(Q[T_{1h}^{n+1}] - Q[T_{2h}^{n+1}]\right)\left(T_{1h}^{n+1} - T_{2h}^{n+1}\right) \geq 0,$$

it follows that

$$\left(T_{1h}^{n+1} - T_{2h}^{n+1}, T_{1h}^{n+1} - T_{2h}^{n+1}\right) \leq \theta \frac{\Delta t}{2} (G_{1h}^{n+1} - G_{2h}^{n+1}, T_{1h}^{n+1} - T_{2h}^{n+1}), \quad (38)$$

using the Young's inequality, we deduce that for all $\epsilon > 0$ we have

$$\begin{aligned} \left(T_{1h}^{n+1} - T_{2h}^{n+1}, T_{1h}^{n+1} - T_{2h}^{n+1}\right) &\leq \theta \frac{\Delta t}{4\epsilon} (G_{1h}^{n+1} - G_{2h}^{n+1}, G_{1h}^{n+1} - G_{2h}^{n+1}) \\ &\quad + \theta \frac{\epsilon \Delta t}{4} (T_{1h}^{n+1} - T_{2h}^{n+1}, T_{1h}^{n+1} - T_{2h}^{n+1}). \end{aligned} \quad (39)$$

By taking $\epsilon = \frac{2}{\theta \Delta t}$, we deduce

$$\left\|T_{1h}^{n+1} - T_{2h}^{n+1}\right\|_{W_h}^2 \leq 2\pi\theta^2 \Delta t^2 \left\|\{I_{1h}\}^{n+1} - \{I_{2h}\}^{n+1}\right\|_h^2. \quad (40)$$

Then

$$\left\|T_{1h}^{n+1} - T_{2h}^{n+1}\right\|_{W_h} \leq 2\pi\theta^2 \Delta t^2 \left\|T_{1h}^{n+1} - T_{2h}^{n+1}\right\|_{W_h}^4. \quad (41)$$

We denote by $B(0, r)$ the closed ball of radius r in W_h where r satisfies

$$r^3 < \frac{1}{8\pi\theta^2 \Delta t^2}. \quad (42)$$

We assume that $T_{1h}^{n+1}, T_{2h}^{n+1} \in B(0, r)$ then we deduce that

$$\left\|T_{1h}^{n+1} - T_{2h}^{n+1}\right\|_{W_h} \leq 8\pi\theta^2 \Delta t^2 r^3 \left\|T_{1h}^{n+1} - T_{2h}^{n+1}\right\|_{W_h}. \quad (43)$$

Let us assume $\left\|g\right\|_{\infty, h}^4 \leq \frac{r}{4C}$, $\left\|I_b\right\|_{\beta, \infty, h} \leq \frac{r}{4C}$ and $\left\|T_{0h}\right\|_{W_h} \leq \frac{r}{2C}$.

Finally $\tilde{\mathcal{H}}_h^n(B(0, r)) \subseteq B(0, r)$ thus $\tilde{\mathcal{H}}_h^n$ is a contraction from W_h to himself. Then, $\tilde{\mathcal{H}}_h^n$ has a unique fixed-point $T_h^n \in W_h$ satisfying the equation (32). Therefore, $\{I_h\}^n = \tilde{\mathcal{H}}_{1h}^n(T_h^n)$ is a unique solution of (31). Hence $(T_h^n, \{I_h\}^n)$ is a unique solution of the system (31)-(32). We proceed iteratively to prove that the map $\tilde{\mathcal{H}}_h^n$ has a unique solution $(T_h^n, \{I_h\}^n)$ for all $n \in \llbracket 0, \dots, N_\tau \rrbracket$. Finally, we conclude that the system (31)-(32) has a unique discrete solution $(T_h^n, \{I_h\}^n)$ for all $n \in \llbracket 0, \dots, N_\tau \rrbracket$. \square

3.2. Stability and error estimate

Let $e_n^h = T(t_n) - T_h^n$ be the error; this is defined at time $t_n = n\Delta t$, for all $n \in \llbracket 0, \dots, N_\tau - 1 \rrbracket$. We note

$$e_{n+\frac{1}{2}}^h = \frac{e_n^h + e_{n+1}^h}{2}$$

does not mean $e^h(n + \frac{1}{2}\Delta t)$.

However, Céa's Lemma asserts that the error of the finite element solution measured in the V-norm is of the same order as the interpolation error, it turns out that the error measured in the H^1 -norm is of the order $O(h^p)$

$$\|T - T_h\|_{H^1(\Omega)} \leq Ch^p \|T\|_{H^{p+1}(\Omega)}, \quad (44)$$

where p is the degree of polynomial approximation and C is a stability and interpolation constant and h denotes the maximum of all element sizes. Furthermore, we have for the error in the L^2 -norm

$$\|T - T_h\|_{L^2(\Omega)} \leq Ch^{p+1} \|T\|_{H^{p+1}(\Omega)}, \quad (45)$$

which means that the convergence rate for the solution itself is $O(h^{p+1})$ [25]. In order to derive a priori estimate for (31) and (32), we shall need the following stability result, for more details see [24, Chapter 13-14].

Lemma 3.4. *Let (T, I) and $(T_h^n, \{I_h\}^n)$ be solutions (15)-(19) and (26),(30), respectively. Then, under the appropriate regularity assumptions for T and I , there exist constants $\Delta t^*, h^* > 0$ and C_T , which depend on τ, Ω and T such that for all $0 \leq \Delta t \leq \Delta t^*$ and $0 \leq h \leq h^*$, we have*

$$\|e_n^h\|_{L^2(\Omega)} \leq C_T (h^{p+1} + \Delta t^2) \quad \forall n \in \llbracket 0, \dots, N_\tau \rrbracket. \quad (46)$$

The proof of Lemma is already essentially covered in the work of V. Thomée [24, Theorem 13.4, p.241].

Let us consider the following norm

$$\|I(t_n) - \{I_h\}^n\| := \left(\sum_{l=1}^{N_\beta} w_l \|I(t_n, \beta_l) - I_h^n\|_{L^2(\Omega)}^2 \right)^{\frac{1}{2}}$$

in \mathbb{V}_h , for all $n \in \llbracket 0, \dots, N_\tau \rrbracket$.

To give an error estimate for the discrete ordinate and the DG method, we introduce the following result given in [16].

Lemma 3.5. *Let us consider the numerical quadrature given by theorem (2.1). We assume that $I \in C(0, \tau; L^2(\Omega, H^s(\mathcal{S}^2)))$, for all $s > 1$. Then, for the discrete-ordinate DG method (25), we have*

$$\|I(t_n) - \{I_h\}^n\| \leq Ch^{p+1/2} \left(\sum_{l=1}^{N_\beta} w_l \|I^l(t_n)\|_{H^1(\Omega)}^2 \right)^{\frac{1}{2}} + C_s m^{-s} \|I(t_n)\|_{L^2(\Omega, H^s(\mathcal{S}^2))},$$

for all $n \in \llbracket 0, \dots, N_\tau \rrbracket$, where C and C_s are a positive constants.

Now in view of the above result, we are ready to prove the following proposition

Proposition 3.6. *Under the hypotheses of Lemma 3.4 and Lemma 3.5, there exist $C_T = C(T) > 0$, $C_{s,\Omega} = C(s, \Omega) > 0$ and $\Delta t^*, h^* > 0$ such that for all $0 \leq \Delta t \leq \Delta t^*$ and $0 \leq h \leq h^*$, we have*

$$\begin{aligned} \left\| I(t_n) - \{I_h\}^n \right\| + \left\| e_n^h \right\|_{L^2(\Omega)} &\leq C_T (h^{p+1} + \Delta t^2) \\ &+ C_{s,\Omega} (h^{p+1/2} + m^{-s}) \left(\left\| T^n \right\|_{H^1(\Omega)}^4 + \left\| g^n \right\|_{H^1(\Omega)}^4 + \left\| I_b^n \right\|_{L^2} \right). \end{aligned}$$

Proof. Let $n \in \llbracket 0, \dots, N_\tau \rrbracket$, $(T_h^n, \{I_h\}^n)$ satisfies (31)-(32). From Lemma 3.4, the inequalities (44) and (45), there exists $C = C(\tau, \Omega, T) > 0$ such that

$$\left\| e_n^h \right\|_{L^2(\Omega)} \leq C_T (h^{p+1} + \Delta t^2)$$

Lemma 3.5 implies

$$\left\| I(t_n) - \{I_h\}^n \right\|^2 \leq Ch^{2p+1} \sum_{l=1}^{N_\beta} w_l \left\| I^l(t_n, \cdot) \right\|_{H^1(\Omega)}^2 + C_s^2 m^{-2s} \|I(t_n)\|_{L^2(\Omega, H^s(\mathcal{S}^2))}^2,$$

then,

$$\begin{aligned} \left\| I(t_n) - \{I_h\}^n \right\| &\leq Ch^{p+1/2} \left(\left\| T^n \right\|_{H^1(\Omega)}^4 + \left\| g^n \right\|_{H^1(\Omega)}^4 + \left\| I_b^n \right\|_{L^2} \right) \\ &+ C_s m^{-s} \|I(t_n)\|_{L^2(\Omega, H^s(\mathcal{S}^2))}, \end{aligned}$$

Finally, there exists $C_{s,\Omega} > 0$ such that

$$\begin{aligned} \left\| I(t_n) - \{I_h\}^n \right\| + \left\| e_n^h \right\|_{L^2(\Omega)} &\leq C_T (h^{p+1} + \Delta t^2) \\ &+ C_{s,\Omega} (h^{p+1/2} + m^{-s}) \left(\left\| T^n \right\|_{H^1(\Omega)}^4 + \left\| g^n \right\|_{H^1(\Omega)}^4 + \left\| I_b^n \right\|_{L^2} \right). \end{aligned}$$

This finished the proof. □

4. Numerical results

In this section, two numerical experiments of our algorithm are presented for solving the coupled equations of heat transfer systems. The main purpose is to illustrate the performances of the proposal method, numerical convergence order, and the number of iterations of the fixed point method.

Given N_τ the number of time step and ϵ the relative error of numerical scheme. The proposed algorithm is given in Algorithm 1. The fixed point iterations and the Newton's method iterations are stopped when the relative error norm is less than $\epsilon = 10^{-6}$. We take the following domain

$$\Omega = \{x = (x, y) \in \mathbf{R}^2; 1 \leq x^2 + y^2 \leq 4, 1 \leq |x| \leq 2 \text{ and } 1 \leq |y| \leq 2\},$$

where this geometry presents the plate of glass after deformation under the effect of high temperature during the thermoforming process of glass, see figure 4.

Algorithm 1 : Numerical Algorithm

```
1: Initializations;
2: for n=0 to  $N_\tau$  do
3:   NormL2=1;
   k=0;
    $T_h^{n+1(0)} = T_h^n$  ;
4:   while NormL2 <  $\epsilon$  do
5:     Solving the full discrete system (31)-(32) // (Newton's method) ;
6:     NormL2 // Relative error;
     k=k+1;
7:   end while
8: end for
```

The nonhomogeneous Dirichlet boundary conditions g is supposed equal to 1 in

$$\Gamma_1 = \{\mathbf{x} = (x, y) \in \mathbf{R}^2; x^2 + y^2 = 1, y \leq 0\}$$

and is equal to 0.5 elsewhere in the boundary. The radiative boundary conditions I_b is assumed equal to g^4 . The initial dimensional condition is assumed equal to

$$T_0(x, y) = (0.25 + 0.2 \times |\sin(2\pi x) \times \cos(2\pi y)|) \quad \forall (x, y) \in \Omega.$$

The first example concerns the following steady radiative conductive heat transfer system:

$$I(\mathbf{x}, \boldsymbol{\beta}) + \boldsymbol{\beta} \cdot \nabla_{\mathbf{x}} I(\mathbf{x}, \boldsymbol{\beta}) = T_g^4(\mathbf{x}) + H_1(\mathbf{x}, \boldsymbol{\beta}) \quad (\mathbf{x}, \boldsymbol{\beta}) \in \mathcal{X} \quad (47)$$

$$-\Delta T_g(\mathbf{x}) + 4\pi\theta T_g^4(\mathbf{x}) = \theta G(\mathbf{x}) + H_2(\mathbf{x}) \quad \mathbf{x} \in \Omega \quad (48)$$

$$T_g(\mathbf{x}) = g(\mathbf{x}) \quad \mathbf{x} \in \Sigma \quad (49)$$

$$I(\mathbf{x}, \boldsymbol{\beta}) = I_b(\mathbf{x}, \boldsymbol{\beta}) \quad (\mathbf{x}, \boldsymbol{\beta}) \in \partial\Omega_-, \quad (50)$$

with the right-hand side function, respectively,

$$H_1(\mathbf{x}, \boldsymbol{\beta}) = \sin(\pi x)\sin(\pi y) + \beta_1 \sin(\pi x)\sin(\pi y) + \beta_2 \sin(\pi x)\cos(\pi y) \\ - \sin^4(2\pi x)\sin^4(2\pi y)$$

and

$$H_2(\mathbf{x}) = 8\pi^2 \sin(2\pi x)\sin(2\pi y) + 4\pi\theta \sin^4(2\pi x)\sin^4(2\pi y) - 4\pi\theta \sin(\pi x)\sin(\pi y).$$

The exact solution of the system is the following:

$$I(\mathbf{x}, \boldsymbol{\beta}) = \sin(\pi x)\sin(\pi y), \quad T(\mathbf{x}) = \sin(2\pi x)\sin(2\pi y).$$

The parameter θ is equal to $\frac{1}{N_s}$ where N_s is the conduction radiation number. We assume that the radiation conduction number N_s is equal to one and the dimensionless final time τ is equal to 0.5. For a deeper discussion of the dimensionless form, we refer the reader to [2] and therein references.

In both examples, we consider the following discretization:

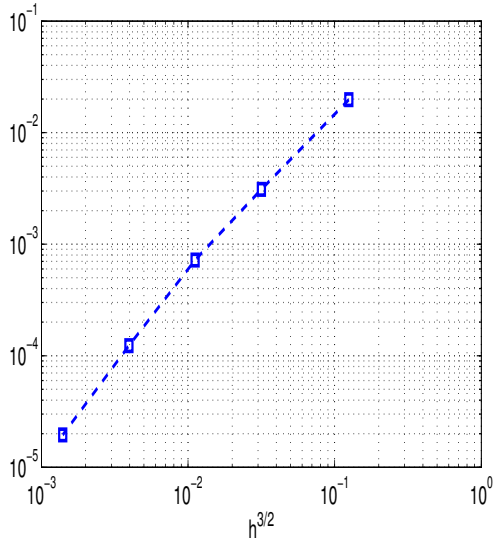
- for the angular variable $\boldsymbol{\beta} = (\boldsymbol{\beta}_1, \boldsymbol{\beta}_2)^T$, we used the S_4 quadrature for the numerical integration on the unit sphere so that there are $N_\beta = 24$ different angular directions, $\{w_l\}_{l=1}^{24}$. In [2] the authors analyze the influence of the numerical quadrature error on the solution accuracy.
- for the time discretization we introduce $\Delta t = \frac{\tau}{N_\tau}$ a time step. The time step Δt must satisfy the constraints (42).
- for the spatial discretization we consider a regular triangulation \mathcal{T}_h of Ω . The parameter h is the diameter of the triangles. The mesh was generated by Freefem++ library¹.

We consider the linear DG element DGP_1 for the numerical approximation of the RTE solution and P_1 piecewise linear continuous elements for CE. Figure 1 shows the evolution of the error in a log scale for problem (47)-(50), confirmed to the order of convergence for the DG and FEM given by Lemmas 3.4 and 3.5. Moreover, figure 2 shows the error of approximation for the coupled system versus h^α where $\alpha = 1.91$. It can be observed that the error of approximation for combined radiative conductive heat transfer system is in order of $O(h^{1.91})$. We now illustrate some numerical results in the case of the transient radiative-conductive heat transfer system. The numerical experience has shown that the fixed point method converges in a very few number of iterations when stability conditions is verified. Figure 3 shows the number of fixed point iterations for two values of Δt ; $\Delta t = 5 \times 10^{-5}$ and $\Delta t = 5 \times 10^{-4}$, and for different values of the space mesh size. It appears that the fixed point method needs two iterations to converge for all space mesh size.

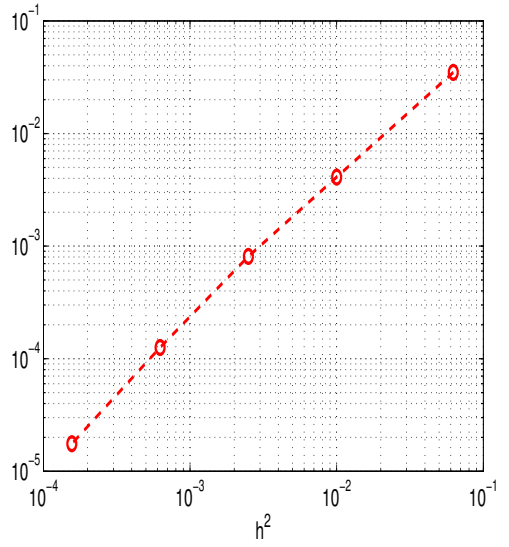
Table 1 shows how often we solve the linear system using LU method with complexity $o(N^2)$ for different value of time and space step ($h, \Delta t$). The integer $N = N_\beta \times (N_\mathcal{T} - N_b) + (N_\mathcal{T} - N_{\partial\Omega})$ is the number of unknowns at each time step. It is clear that the total number of resolution of the linear system needed for the convergence of the algorithm strongly depends on the time step.

In Figure 4, we plot the fields of the temperature of the reference solution for final time $\tau = 0.5$ and with a refined mesh size $h = 1.25 \times 10^{-2}$ and $\Delta t = 10^{-5}$. However, in [2], several physical cases with different types of boundary conditions (nonhomogeneous Dirichlet and Robin Conditions) and with a comparison of our numerical code to results are presented in [26].

¹<http://www.freefem.org/>



(a) Error $\|I - I_h\|_h$ vs $h^{3/2}$



(b) Error $\|T - T_h\|_{L^2(\Omega)}$ vs h^2

Figure 1: Error of approximations of DG and FEM for solving (47)-(50)

h	Δt	# LU numerical resolution of the linear system
h=1/10	$5 \cdot 10^{-4}$	1768
	10^{-4}	8043
	5×10^{-5}	15418
h=1/20	5×10^{-4}	1772
	10^{-4}	8061
	5×10^{-5}	15422
h=1/40	5×10^{-4}	1775
	10^{-4}	8066
	5×10^{-5}	15428
h=1/80	5×10^{-4}	1775
	10^{-4}	8066
	5×10^{-5}	15435

Table 1: Complexity of the Algorithm 1 for solving the coupled radiative conductive heat transfer system for the dimensionless final time $\tau = 0.5$.

5. Conclusion

In this paper, we studied discrete-discontinuous and continuous Galerkin methods combined with the stable Crank-Nicolson scheme for solving the radiative-conductive heat transfer system. The existence and uniqueness result of the

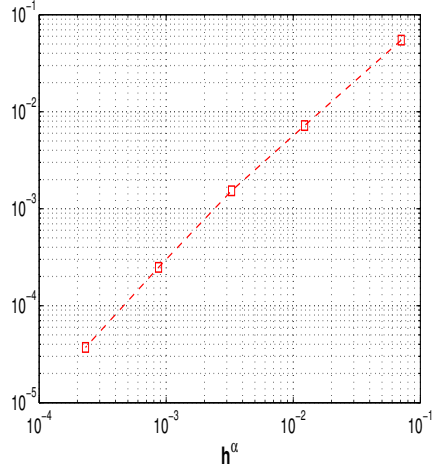
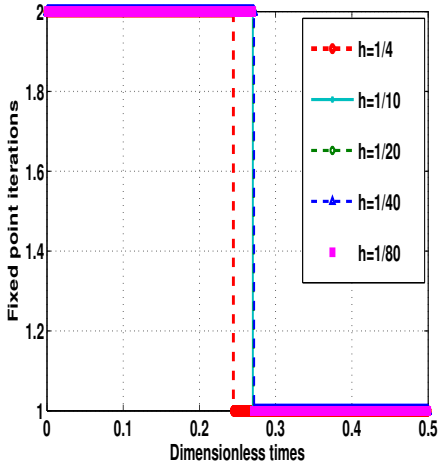
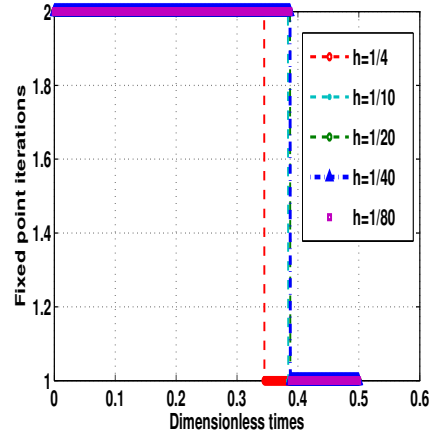


Figure 2: $\|I - I_h\|_h + \|T - T_h\|_{L^2(\Omega)}$ vs h^α where $\alpha = 1.91$.



(a) $\Delta t = 5 \times 10^{-5}$



(b) $\Delta t = 5 \times 10^{-4}$

Figure 3: Numbers of iterations of fixed point method for different dimensionless times.

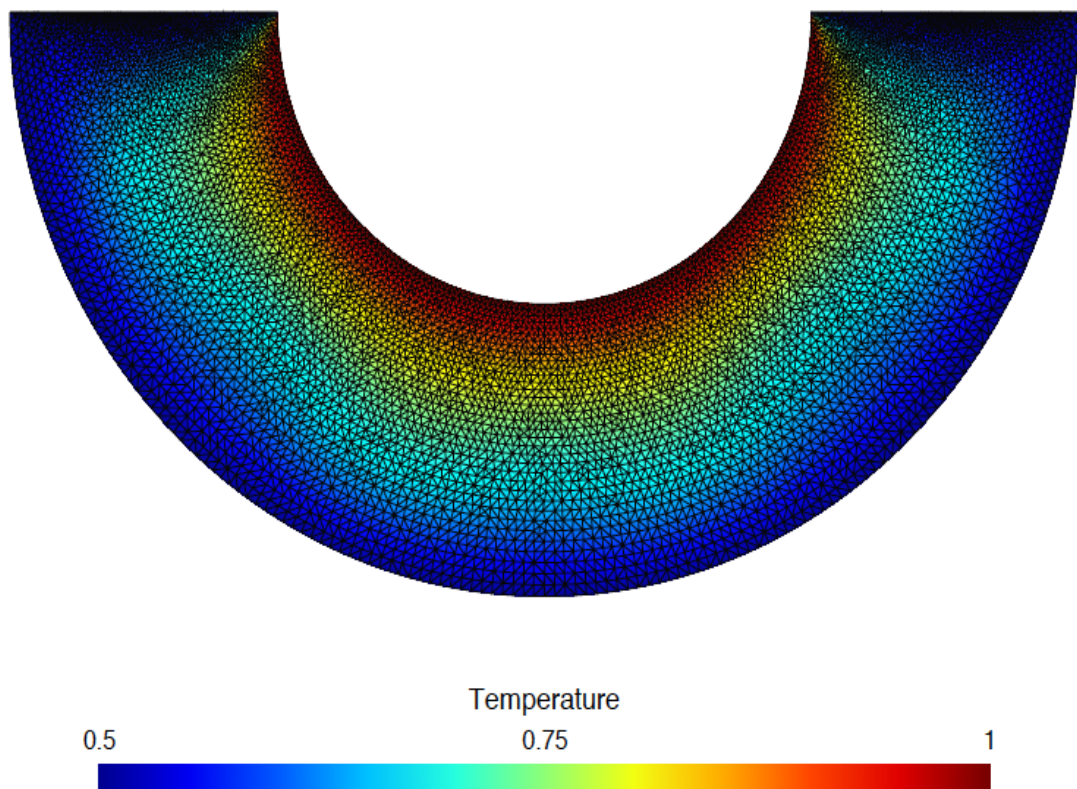


Figure 4: The field of the temperature for dimensionless final time $\tau = 0.5$ and the mesh size $h = 1.25 \times 10^{-2}$ and time step $\Delta t = 5 \times 10^{-5}$.

solution for the continuous and full discrete radiative conductive heat transfer system is established. Finally, a stability and error analysis of the numerical methods are performed. Our analysis gives explicitly how to choose the time step Δt and mesh size h to achieve convergence when the initial and boundary data satisfies the given constraints. Some numerical examples are included to demonstrate the convergence behavior of the methods. In practice when stability constraints are verified a few number of fixed point iteration are needed to have numerical convergence. To compare DG-FEM with FEM-FEM and FVM-FEM for solving the radiative-conductive heat transfer system, for instance, be of crucial relevance to examine the accuracy of our method. One of the topics of future research will be to explore this issue.

Acknowledgements: We would like to thank the **CAM corresponding editor** and the anonymous **referees** for their suggestions which led to the improvement of the original manuscript.

References

- [1] M. Ghattassi, J.R. Roche, and D. Schmitt, Existence and uniqueness of a transient state for the coupled radiative-conductive heat transfer problem, to appear, *Computers and Mathematics with Applications*, (2018).
- [2] M. Ghattassi, J.R. Roche, F. Asllanaj and M. Boutayeb, Galerkin method for solving combined radiative and conductive heat transfer, *International Journal of Thermal Sciences* 102 (2016)122-136.
- [3] M., Ghattassi, M., Boutayeb, J.R. Roche, Reduced order observer of a finite dimensional radiative-conductive heat transfer systems, accepted *SIAM (sicon)*, 2018.
- [4] D. A. Pietro and A. Ern, *Mathematical Aspects of Discontinuous Galerkin Methods*, Springer, 2011.
- [5] P. Nelson, Convergence of the discrete ordinates method for anisotropically scattering multiplying particles in a subcritical slab, *SIAM J. Numer. Anal.*, 10 (1973) 175-181.
- [6] P. Nelson and H. D. Victory, Theoretical properties of one-dimensional discrete ordinates, *SIAM J. Numer. Anal.*, 16 (1979) 270-283.
- [7] M. Jing, S. Ya-song and L. Ben-Wen, Simulation of combined conductive, convective and radiative heat transfer in moving irregular porous fins by spectral element method, *International Journal of Thermal Sciences*, 118 (2017) 475-487.
- [8] C. Shang-Shang, L. Ben-Wen and S. Ya-Song, Chebyshev collocation spectral method for solving radiative transfer with the modified discrete ordinates formulations, *International Journal of Heat and Mass Transfer*, 88 (2015) 388-397.
- [9] S. Ya-Song and L. Ben-Wen, Spectral collocation method for transient combined radiation and conduction in an anisotropic scattering slab with graded index, *Journal of Heat Transfer*, 24(4) (2010) 823-832.
- [10] M. Jing, S. Ya-song and L. Ben-Wen, Spectral collocation method for transient thermal analysis of coupled conductive, convective and radiative heat transfer in the moving plate with temperature dependent properties and heat generation, *International Journal of Heat and Mass Transfer*, 114 (2017) 469-482.
- [11] P. Lesaint and P. A. Raviart, On a finite element method for solving the neutron transport equation, in *Mathematical Aspects of Finite Elements in Partial Differential Equations*, C. de Boor, ed. Academic Press. New-York.p. 89-123, 1974.
- [12] E. W. Larsen and P. Nelson, Finite-difference approximations and super convergence for the discrete ordinate equations in slab geometry, *SIAM J. Numer. Anal.*, 19 (1982) 334-349.
- [13] J. Pitkaranta and R. R. Scott, Error estimates for the combined spatial and angular approximations of the transport equation in slab geometry, *SIAM J. Numer. Anal.*, 20 (1983) 922-950.

- [14] M. Asadzadeh, Analysis of a fully discrete scheme for neutron transport in two-dimensional geometry, *SIAM Journal on Numerical Analysis*, 23 (1986) 543-561.
- [15] M. Asadzadeh, L^p and eigenvalue error estimates for the discrete ordinates method for two-dimensional neutron transport, *SIAM J. Numer. Anal.*, 26 (1989), 66-87.
- [16] W. Han, J. Huang, and J. A. Eichholz, Discrete-ordinate discontinuous Galerkin methods for solving the radiative transfer equation, *SIAM J. Sci. Comput.*, 32 (2010) 477-497.
- [17] F. Brezzi, J. Rappaz, and P. Raviart, Finite-dimensional approximation of nonlinear problems. Part I braches of nonsingular solutions, *Numer. Math.*, 36 (1980) 1-25.
- [18] K. Chrysafinos and L. S. Hou, Error estimates for semi discrete finite element approximations of linear and semilinear parabolic equations under minimal regularity assumptions, *SIAM Journal on Numerical Analysis*, 40 (2002) 282-306.
- [19] X. Feng and Y. He, Convergence of the Crank-Nicolson/Newton scheme for nonlinear parabolic problem, *Acta Mathematica Scientia*, 36 (2016) 124-138.
- [20] S.G. Mikhlin, *Multidimensional Singular Integrals and Integral Equations*, Pergamon Press, Oxford, 1965.
- [21] M. F. Modest, *Radiative Heat Transfer*, Academic Press, 2003.
- [22] F. W. Freeden, T. Gervens, and M. Schreiner, *Constructive Approximation on the Sphere with Applications to Geomathematics*, Oxford University Press, Oxford, 1998.
- [23] K. K. Hesse and I. H. Sloan, Cubature over the sphere S_2 in sobolev spaces of arbitrary order, *J. Approx. Theory*, 141 (2006) 118-133.
- [24] V. Thomée, *Galerkin Finite Element Methods for Parabolic Problems*, Vol 25. Springer Series in Computational Mathematics. Springer-Verlag, Berlin, second edition, 2006.
- [25] P. G. Ciarlet, *The Finite Element Method for Elliptic Problems*, Society for Industrial and Applied Mathematics, 2002.
- [26] F. Asllanaj, G. Parent, G. Jeandel, Transient Radiation and Conduction Heat Transfer in a Gray Absorbing-Emitting Medium Applied on Two-Dimensional Complex-Shaped Domains, *Numerical Heat Transfer, Part B: Fundamentals* 52(2)(2007) 179-200.